Speed Control of Drive Unit in Four-rotor Flying Robot

Stanisław Gardecki, Wojciech Giernacki and Jarosław Gośliński
Institute of Control and Information Engineering, Poznan University of Technology, 3a Piotrowo St., Poznan, Poland

Keywords: UAV, Four-rotor Flying Robot, Speed Control of Drive Unit, Coefficient Diagram Method.

Abstract: In this paper the synthesis of speed controller for drive unit is presented. Its aim is to generate the lift force of multi-rotor flying robot. Parameters of drive unit model were experimentally determined based on recorded time characteristics from engine test stand. The use of two alternative controllers: CDM and PID types was proposed. The CDM controller was tuned in accordance with the Coefficient Diagram Method and the PID controller in MATLAB's Simulink Response Optimization tool. The efficiency of both types control systems was compared for specified conditions. Integral quality indices were adopted as a measure of assessment. Obtained simulation results were discussed in the context of implementation on a real robot.

1 INTRODUCTION

Many concepts of unmanned aerial vehicles have been already developed. Usually these robots are used in tasks of observation, patrolling and recognition in areas of military and civil (Gertler, 2012), as well as in the science and entertainment (Augugliaro et al., 2010). The use of several drive units, often embedded in the same plane, is their similarity. Such a solution (without the control of angle of blades attack as it is in helicopters) results with the stiff construction of whole robot, but it enforces a specific control – change of the robot's position and movement is only an effect of the speed change of appropriate drive unit (DU) - obtained from the onboard microcontroller, which aim is to split the thrust into particular drives. A thinking oriented to obtainment of the simplest possible mechanical construction supported with advanced computational unit and onboard sensors, works well in four-rotor flying robots, but only with effective control techniques (Gardecki and Kasiński, 2012).

In this paper, attention was focused on the synthesis of variable speed control of one DU (described in detail in Gardecki and Kasiński, 2012) with the brushless DC motor and by the not well known algorithm of the Coefficient Diagram Method (CDM) (Manabe, 1998), which has been already applied with success within the context of avionics (Budiyono, 2005). The proposed CDM controller is an alternative to commonly used PID (Salih et al., 2010). The avionics of considered robot from Fig. 1 equipped with four DUs (Fig. 2) involves the use of two control loops – the external (slower) to control movement and orientation of robot by the board controller, as well as the inner loop for variable speed control of each of four DUs. The determina-tion of rotational speed is conducted by the change of voltage signal fulfillment - PWM (Pulse-Width Modulation) on particular DU controller input.

Figure 1: Hornet robot.

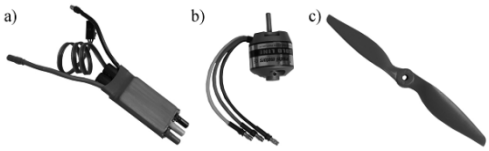

Figure 2: Speed controller (a), drive unit: brushless DC engine (b) and propeller (c).

The CDM control according with the idea of robust control does not enforce to obtain complica-ted and complex mathematical model of the DU, but only the simplest possible description, which accura-tely

Gardecki S., Giernacki W. and Goslinski J..
Speed Control of Drive Unit in Four-rotor Flying Robot.
DOI: 10.5220/0004477002450250
In *Proceedings of the 10th International Conference on Informatics in Control, Automation and Robotics* (ICINCO-2013), pages 245-250
ISBN: 978-989-8565-71-6

reflects the dynamics. The aim of control algorithm is then (in addition to stability and good quality of control providing) a correction of impact of nonmodeled and missed part of plant's dynamics – therefore it was decided to use the experimental method for determining DU's model parameters from its step response to the transfer function form.

2 ENGINE TEST STAND

For tests of high speed drive units, a special test stand (TS) was built (Fig. 3), which enabled remote control and measurements. In order to provide constant and stable power supply to the DU, the inRadio IN-450 power supply with high current efficiency may be used, but during tests controller drew power from 6000 mAh 11,1 V battery. The TS was equipped with a set of sensors which allow to control the power supply voltage of controller and to measure of the DU current consumption, generated thrust by the set of engine/propeller and the rotational speed. The data from measurement system were transmitted as a report to the computer application, which was used as an setpoint adjuster and controller (to set the same experimental conditions for various power units). The signal sampling frequency was equal to 300 Hz.

On the basis of earlier tests (Gardecki and Kasiński, 2012) it was observed that despite the use of the same BLDC engines and propellers, recorded characteristics of drive units differ from each other, which leads to stabilization difficulties of the robot during the flight and reduces the flight time by unfairly increase consumption of electricity. On this reason authors opted for the synthesis of control systems (with PID and CDM type controllers) for particular DU. This paper considered results of tuning for an exemplary, one of four drive units.

Two tests to provide a maximum knowledge about modeled object were conducted. In the first study, by the change of set voltage (fulfilment of PWM) fed to the engine (in range from 0 to 100%, step equal to 1%), characteristics of signals shown in Fig. 4, were recorded. For the mass of the quadrotor equal to 1,6 kg, the necessary and total thrust which allows to overcome its force of gravity amounts 15,696 N. It should be noted that the maximum thrust (19,09 N) of the tested DU is achieved at PWM=77 %, RPM=8893 r/min and the current is equal to I=15,551 A, but the maximum speed RPM=9039 r/min is achieved at PWM=75 %, and I=14,419 A. These parameters illustrate limits of useful ranges during the operation of robot.

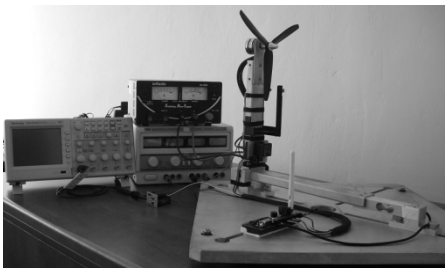

Figure 3: Engine test stand.

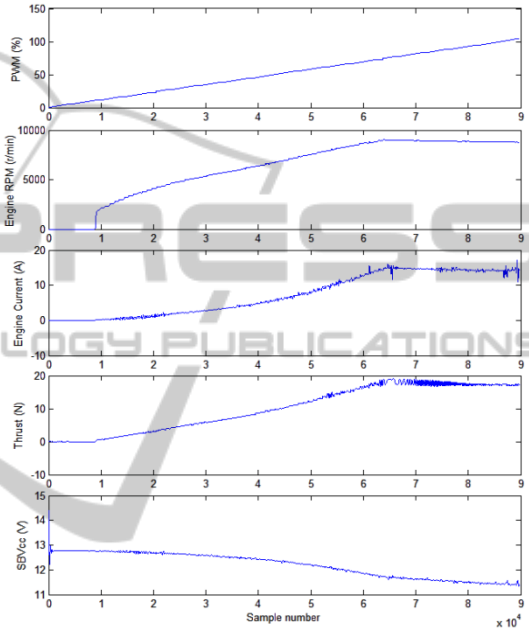

Figure 4: PWM (a), propeller rotational speed – RPM (b), engine current (c), thrust of engine/propeller unit (d), power supply voltage (e) in the function of control voltage change from 0 to 5 V.

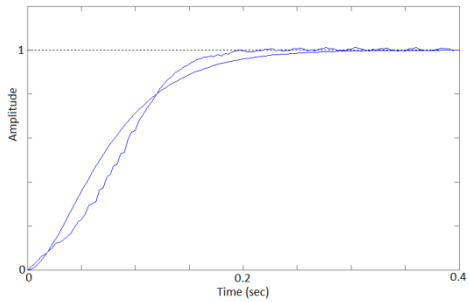

Figure 5: Model (smooth line) and robot step responses matching.

In the second test a step response of modeled DU has been observed (voltage changed from 0% to 100% PWM) to obtain the simplest plant model, which is desirable for control system synthesis, but it has to accurately reflect the particular DU dynamic,

which useful thrust starts from minimum value 3,924 N (RPM=4492,5 r/min). The time course of rotational speed from Fig. 5 has been recorded and it was decided to apply the second-order inertial plant model (1), which parameters were determined by step responses matching in experimental way.

$$G(s) = \frac{1}{(0,04s+1)^2} = \frac{1}{0,0016s^2 + 0,08s + 1} \quad (1)$$

3 SYNTHESIS OF CDM AND PID CONTROLLERS

CDM Control

The CDM algorithm is based on an idea of the use of relationship between obtained closed-loop system time characteristics and the placement of its characteristic polynomial poles on the complex plane *s* (Manabe, 1998). The control system under consideration is presented in Fig. 6, where *F(s)* - input numerator polynomial of controller transfer function, *A(s)/B(s)* - numerator/denominator polynomial of controller transfer function, *N(s)/D(s)* - numerator/denominator of plant transfer function, *r(t)/y(t)* - reference/output signal, *e(t)* - control error, *z(t)* - external disturbance signal, *v(t)/u(t)* - un/constrained control signal, *m(t)* - measured noise signal. A characteristic polynomial of closed-loop system *P(s)* (of *n*-th degree) is defined by the equation (2):

$$P(s) = D(s)A(s) + N(s)B(s) = \sum_{i=0}^{n} a_i s^i, \quad (2)$$

The synthesis of controller for system from Fig. 6 (with the use of CDM algorithm from Fig. 7) and CDM procedure (Hamamci and Koksal, 2004) are presented below.

A. Controller Synthesis

- Notation of Plant Model with use of transfer Function:

$$\frac{N(s)}{D(s)} = \frac{n_l s^l + n_{l-1} s^{l-1} + \ldots + n_1 s + n_0}{d_m s^m + d_{m-1} s^{m-1} + \ldots + d_1 s + d_0}, \quad (3)$$

where: *l* – degree of *N(s)* polynomial (less or equal to *m* – degree of *D(s)* polynomial).

- Choice of Controller Structure

Based on analysis of expected disturbances, degrees of polynomials *A(s)* and *B(s)* are chosen according to Table 1. Controller polynomials, respectively degree: *p* and *q* are written in forms (4):

$$A(s) = \sum_{i=0}^{p} l_i s^i, \quad B(s) = \sum_{i=0}^{q} k_i s^i. \quad (4)$$

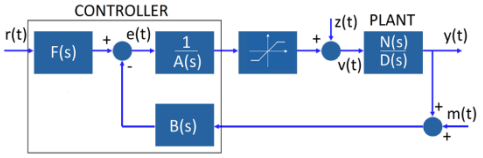

Figure 6: Block diagram of CDM control closed loop.

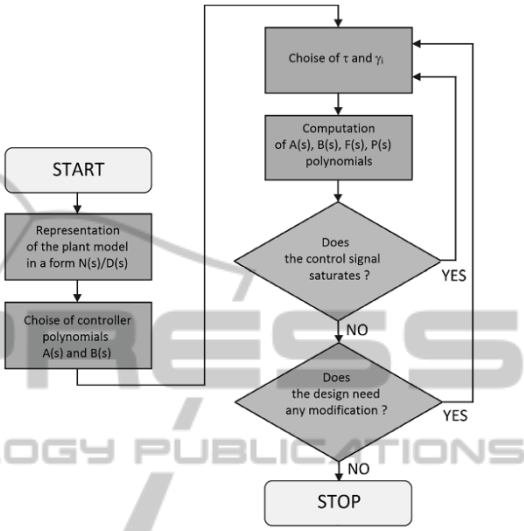

Figure 7: CDM algorithm.

Table 1: The choice of transfer function polynomials degrees due to expected type of disturbances.

Type of disturbance	Degree of *A(s)*	Degree of *B(s)*	Degree of *P(s)*	Condition
None	*m-1*	*m-1*	*2m-1*	-
Step	*m*	*m*	*2m*	$l_0=0$
Ramp	*m+1*	*m+1*	*2m+1*	$l_0= l_1=0$
Impulse/ sinusoidal	*m-1*	*m-1*	*2m-1*	-

- Choice of τ and γ_i Values

The CDM uses relationship (5) between the equivalent of time constant (τ) – used to build the characteristic polynomial (P_T) and the expected time of step response (t_s):

$$\tau = t_s / (2,5 \sim 3). \quad (5)$$

The advantage of proposed algorithm is Manabe standard form (6) (vector specifying stability indices - γ_i). It represents system stability on a Coefficient Diagram (CD) and defines the $P_T(s)$, which should be used to ensure requirements of system dynamics in the first iteration of algorithm. Standard forms should be treated as initial setting values of each index of stability - details in (Manabe, 1998).

$$\underline{\gamma_i} = [2,5 \quad 2 \quad 2 \quad \ldots \quad 2]^T \quad (6)$$

for $i=1,\ldots,n-1$; $\gamma_0=\gamma_n=\infty$ and n is $P_T(s)$ degree.

To specify numerically and graphically (on CD) stability limit of system, equation (7) for stability limits is used:

$$\gamma_i^* = \frac{1}{\gamma_{i-1}} + \frac{1}{\gamma_{i+1}}. \quad (7)$$

- Calculation of $P(s)$, $F(s)$, $A(s)$ and $B(s)$

The equivalent of time constant and stability indices building the target characteristic polynomial (8), which is compared to equation (2), therefore from diophantine equation (9) numerical values of controller coefficients (l_i and k_i) may be calculated.

$$P_T(s) = a_0 \left\{ \left[\sum_{i=2}^{n} \left(\prod_{j=1}^{i-1} \frac{1}{\gamma_{i-j}^{j}} \right) (\tau s)^i \right] + \tau s + 1 \right\} \quad (8)$$

$$P(s) = P_T(s) \quad (9)$$

Polynomial $F(s)$ is defined by the equation (10):

$$F(s)\big|_{s=0} = \left. \frac{P(s)}{N(s)} \right|_{s=0}. \quad (10)$$

- Recurrence of CDM Algorithm

The option of procedure recurrence depends only on the fact, whether a satisfactory control quality was obtained (according to previously chosen criterion *e.g.* size of the overshoot, saturation of control signal, settling time of output signal, specified limit of stability). By reduction of stability limit or extension of the expected time of step response, algorithm may be recurred. The CD analysis is useful in this part of procedure.

B. Coefficient Diagram

In synthesis and analysis of the control system based on the CDM algorithm, half-logarithmic coefficient diagram is used (Fig. 8), where the vertical axis logarithmically shows coefficients of the characteristic polynomial (a_i), stability indices (γ_i), stability limits (γ_i*) and the equivalent time constant (τ), while the horizontal axis shows the i values corresponding to each coefficient.

In Fig. 8 number marks were introduced:

- numerical values (a_i) of $P_T(s)$ coefficients – *I*,
- numerical values of stability indices (γ_i) – *II*,
- numerical values (k_i) of $B(s)$ coefficients– *III*,
- equivalent of time constant (τ) – *IV*,
- numerical values of stability limits (γ_i*) – *V*.

By analogy with the Bode and Nyquist plots, coefficient diagram provides the necessary information about the system robustness, stability and dynamics. The degree of convexity, which is obtained from coefficients of the characteristic polynomial, gives a measure of stability, while the general inclination of the curve gives a measure of the speed of response (Manabe, 1998). The variation of the shape of the a_i curve due to plant parameter variation is a measure of robustness (Hamamci and Koksal, 2004).

Stability analysis

For values γ_i and γ_i^* vertical distance between the *II* and *V* curves is a measure of system stability (if the distance for each i increases, then the system has bigger stability limit). Analyzing the situation in the complex plane s, this corresponds to the placement of system poles in the left half-plane in larger distance from the imaginary axis specifying the limit of stability. It should be noted that the system is stable only if curves do not cross each other and the curve *II* is above the curve *V* (Manabe, 1998). The basis of a theoretical analysis of a system stability is Lipatov and Sokolov criterion.

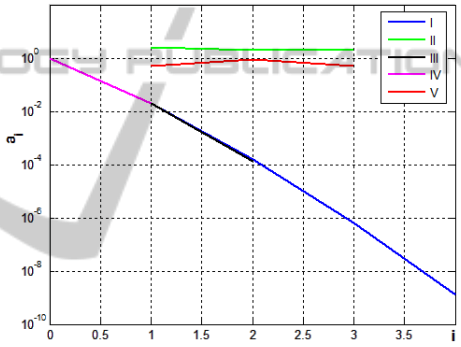

Figure 8: Coefficient diagram of CDM system model (1).

Robustness

Assessment of system robustness is based on the mutual position of *I* and *III* curves. If the curve *III* is below the curve *I*, then the system is more robust to parametric uncertainty – robustness increases when the curves are closer to each other. It was shown in (Manabe, 2010) that depending on the plant type, in general, it is possible to design with the use of CDM algorithm a control system, which is stable due to the change the i-th characteristic polynomial coefficient values in the range from 0,5 to 3 times in relation to the nominal value of this factor.

Dynamics

Dynamics of system is characterized by the time constant equivalent. The system is characterized by higher dynamics for smaller values of τ - in diagram it corresponds to a larger angle of the curve *IV* inclination. Analysis of the time constant equivalent is also important in the case of control signal constraints. If the control signal is saturated, then the

key issue in the control system synthesis is to return to the stage of selection of expected equivalent time constant value to increase this value (to slow down the expected step response) and retry the algorithm.

The CDM controller was tune for possibility of step type disturbance appearance (*eg.*, blow of the strong wind on the DU propellers). After the selection of appropriate controller structure (according to the Table 1) for the model transfer function, the Manabe standard form (6) was assumed. Then for the chosen (expected) step response time t_s=0,05 ~0,06 sec, equivalent of time constant τ=0,02 sec was calculated. The CDM controller was obtained:

$$\begin{aligned} A(s) &= 0,0008s^2 + 0,36s, \\ B(s) &= 0,0001s^2 + 0,0196s + 1, \\ F(s) &= 1. \end{aligned} \tag{11}$$

PID Control

To compare the control and tracking quality, the second controller (PID - proportional-integral-derivative), was used. Its parameters, namely the gain of proportional part (k_P), integral part (k_I) and derivative part (k_D), were set in Simulink Response Optimization tool – for similar assumptions as for the CDM control. The optimization algorithm found solution after 97 iterations (different controller sets) as: k_P=3,24, k_I=49,40, k_D=0,06. This controller provides a step response after the time ~ 0,06 sec with minimal overshoot (Fig. 9).

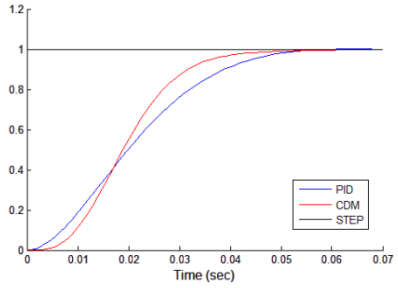

Figure 9: Step responses for CDM and PID controllers.

4 COMPARATIVE TESTS

Presented above control systems have been implemented in the MATLAB 7.0/ Simulink under OS Windows 7 system in default configuration. Obtained results from numerical tests are presented below. Parameters of PID and CDM control systems remained constant in all performed tests. To control quality assessment of the DU speed, except time characteristics, integral quality indices were used: IAE (integral of absolute value of error) and ISE (integral of error squared).

Tracking of Setpoint Signal in Nominal Systems

In the first stage of numerical tests, in systems without disturbances and constraint of control signal amplitude, tracking quality of set rectangular signal (amplitude equal to 1, period to 0,8 sec, control horizon to 2 sec), was tested. Signals are presented in Fig. 10 and values of integral quality indices are:
- 1,925 (IAE) & 1,896 (ISE) for CDM,
- 1,903 (IAE) & 1,869 (ISE) for PID system.

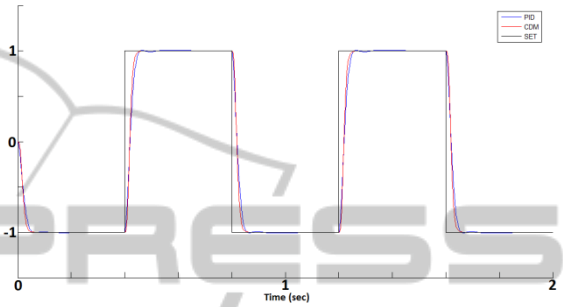

Figure 10: Tracking of SET (setpoint) signal in PID and CDM nominal systems.

The analysis of signals (Fig. 10) informs that despite the use of optimization procedure to obtain the PID controller and fulfilment of assumptions imposed on the step response (Fig. 9), as well as marginally lower values of IAE and ISE indices – PID controller has an undesirable tendency to over-shoot, which is not present in CDM control.

Tracking of Setpoint Signal at Constraints

In the second simulation test one imposed in both control systems the same saturation of control signal amplitude (u_{max}=±6). All simulation parameters and controllers remain unchanged in the relation to the first test. The results are presented in the form of reference and output signals (Fig. 11). Integral quality indices were recorded and are equal respectively to 1,968 (IAE) & 2,043 (ISE) for CDM and 1,942 (IAE) & 1,963 (ISE) for PID controller.

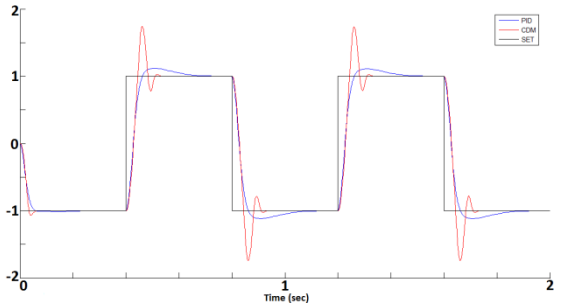

Figure 11: Tracking of SET (setpoint) signal in PID and CDM nominal systems at constraints - u_{max}=±6.

Despite the fact that IAE and ISE values are similar for both controllers, the analysis of Fig. 11 shows the differences in time curves of both output signals – in the case of ideal (nominal) control system with constraint of control signal amplitude – PID controller produces significantly less overshoot, but it needs almost twice as much time to bring output signal value to the level of reference signal.

Tracking of Setpoint Signal in disturbed Systems at Constraints

In the last test, an additional external disturbance with step change of amplitude level over the time, has been introduced to CDM and PID systems. The quality of tracking was verified in the simulation with similar parameters as in previous test. Values of integral quality indices are equal respectively to 1,969 (IAE), 2,046 (ISE) for CDM controller and 1,995 (IAE), 2,082 (ISE) for PID. Results of simulations (with external disturbance signal – DIST) are presented in Fig. 12. In both cases, the systems follow a setpoint signal, but for the CDM control, the quality is definitely better – appearing disturbances are damped much more quickly.

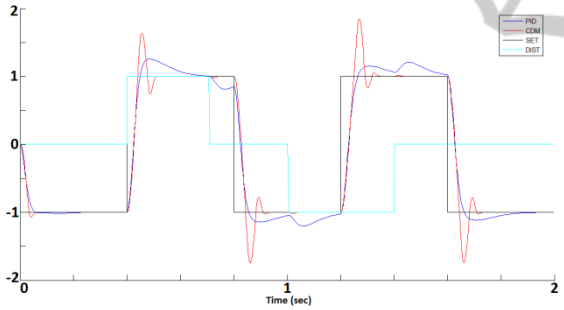

Figure 12: Tracking of SET (setpoint) signal in PID and CDM disturbed systems at constraints - $u_{max}=\pm 6$.

5 CONCLUSIONS

Evaluation of the both presented control techniques efficiency for variable speed control of the flying robot DU is not easy and unambiguous, because of robot's control specificity as a complex dynamic object. Its speed control is directly associated with position and orientation, provided by the external cascade controller which supports all four engines.

In planning of the minimum cost of energy (minimizing the control signal changes frequency), which is important from the perspective of the limited length of flight (approx. 15 minutes) by the battery power supply used in robot, it is reasonable to select the PID controller, because it generates a smooth transfer characteristics. The tendency to overshoot can be eliminated by different method of tuning than suggested in this article, such as swarm optimization algorithm or genetic algorithms.

On the other hand so dynamic object as quadrotor is very sensitive to transient environmental conditions, such as wind and roll and it requires very fast reactions. The CDM controller, which is designed for the presence of step type disturbances, during the third conducted test ensured generally faster damping of disturbance effects as well as better tracking quality through dynamic changes of control signal. The overshoot that appears, should be eliminated by the use of modified algorithm of the CDM method. Such works had been already conducted with the positive effects for other types of objects – by using an additional block of pre-filter in the controller, which parameters may be optimized by the pole-colouring method (Bir et al., 2005).

The use of above proposed techniques of the PID and CDM controller sets improvement is now a starting point for further researches and implementation tests on the real robot.

REFERENCES

Augugliaro, F., D'Andrea, R., Lupashin, S. and A. Schöllig, 2010. Synchronizing the Motion of a Quadrocopter to Music. In *Proc. of the IEEE Inter. Conf. on Robotics and Aut.*, Alaska, pp. 3355 – 3360.

Bir, A., Öcal, Ö. and M. T. Söylemez, 2005. Robust Pole Assignment using Coefficient Diagram Method. In *Proc. of ACSE'05 Conf.*, Cairo, Egypt, CD.

Budiyono, A., 2005. Onboard Multivariable Controller Design for a Small Scale Helicopter Using Coefficient Diagram Method. *In Proc. of the ICEST*, Seoul, CD.

Gardecki, St. and A. Kasiński, 2012. Testing and selection of electrical actuators for multi-rotor flying robot, *Measurements, Automation & Control*, vol. 1, no. 1, pp. 80-83.

Gertler, J., 2012. *U. S. Unmanned Aerial Systems*, Congressional Research Service Report, USA.

Hamamci, S. E. and M. Koksal, 2004. A Program for the Design of Linear Time Invariant Control Systems: CDMCAD. *Computer Applications in Engineering Education*, vol.12, no.3, pp. 165-174.

Manabe, S., 1998. Coefficient Diagram Method. In *Proc. of IFAC Automatic Control in Aerospace*, Seoul, pp. 199-210.

Manabe, S., 2010. *Coefficient Diagram Method for Control system design*, unpublished part of the monograph provided by author.

Salih, A. L., Moghavvemi, M., Mohamed, H. A. F. and K. S. Gaeid, 2010. Flight PID controller design for a UAV quadrotor. *Scientific Research and Essays*, vol. 5, no. 23, pp. 3660-3667.